

# Dependence of Solar Cell Contact Resistivity Measurements on Sample Preparation Methods

Andrew M. Gabor<sup>1</sup>, Geoffrey Gregory<sup>2</sup>, Adam M. Payne<sup>3</sup>, Rob Janoch<sup>1</sup>, Andrew Anselmo<sup>1</sup>, Vijay Yelundur<sup>3</sup>, Kristopher O. Davis<sup>2</sup>

<sup>1</sup> BrightSpot Automation LLC, Westford, MA, USA

<sup>2</sup> Florida Solar Energy Center - University of Central Florida, Orlando, FL, USA

<sup>3</sup> Suniva Inc, Norcross, GA, USA

**Abstract** — The measurement of contact resistivity between the grid metallization of a solar cell and the underlying silicon wafer is most conveniently performed by cutting strips from solar cells rather than fabricating dedicated structures with variable spaced contacts. We studied the effect of strip width on the measurements and found the lowest values in the range of 10-15 mm. We found laser scribing conditions whereby strips could be successfully isolated on the emitter side without snapping strips from the rest of the cell.

## I. INTRODUCTION

The contact resistivity  $\rho_C$  (also called the specific contact resistance) between the metal contacts of crystalline silicon solar cells and the underlying silicon wafers is of critical importance to the efficiency of the cells. While the photovoltaics literature has many reports of using strips cut from cells for contact resistivity measurements, there is little reported concerning the methods to prepare the strips and the effects of variables such as strip width and finger conductivity. In this paper we explore the effect of strip width and the strip preparation method in an effort to improve the accuracy, convenience, and value of the measurements.

## II. BACKGROUND

In general, two routes are taken when studying the contact resistivity by the traditional TLM method [1-5]. One method is to fabricate separate structures that are processed similarly to the standard cells, but which have an array of variably spaced contacts instead of a standard grid. By measuring the resistance between the variable spaced contacts, the resistance can be plotted vs. the contact spacing and from this curve the contact resistance  $R_C$  and the sheet resistance  $\rho_{SH}$  between the contacts can be extracted. Current crowding effects are common whereby more current transfers from the contact to the silicon near the edge of the contacts than in the middle, and the analysis of the plot can also yield the characteristic width of the contact over which the current transfers called the transfer length  $L_T$ . For contacts of length  $W$ , one can multiply  $R_C$  by the “utilized” area of the contact ( $W \times L_T$ ) to yield  $\rho_C$  with units of ohms-cm<sup>2</sup>.

This approach of fabricating separate structures is inconvenient, and thus a more commonly utilized method in the industry is to cut strips (of width  $W$ ) from standard cells and achieve the variable spacing by skipping over steadily increasing numbers of intermediate finger (contact) segments. Most commonly, the concept of transfer length is ignored, and rather researchers report an effective contact resistivity  $\rho_{C-eff}$  by using the full width  $f$  of the fingers in the calculation. By using actual cells, the measurement finds application not just in experiments, but also for quality control in cell factories. Even though the test is inherently destructive, pieces of cells that are broken after the metallization firing step can be used to eliminate the impact on factory yield.

Most groups have historically performed this measurement of  $\rho_C$  by hand placing one pair of current and voltage probes fixed on one finger segment, and moving the other pair to the other fingers and recording the voltage drop at a fixed current. Challenges with the manual method are 1) the difficulty in probing narrow fingers by hand, 2) the time consuming nature of the measurement, 3) errors introduced by ambient light, and 4) errors introduced by inconsistent placement of the probes. It is possible to automate this method, and we have previously reported [1] on our semi-automatic tool, the *ContactSpot*, to perform this measurement. Fig. 1 shows a photo of two *ContactSpot* units, one with the cover closed. Fig. 2 demonstrates the usefulness of the tool with a plot of the median  $\rho_{C-eff}$  and  $\rho_{SH}$  values across strips from full cells for a Suniva experiment in which the P implant dose was varied.



Fig. 1. *ContactSpot* tools for measuring contact resistivity

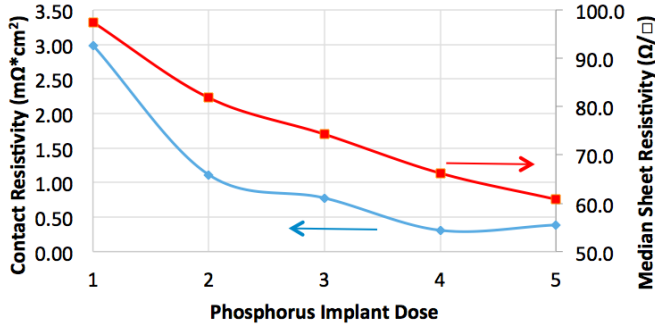


Fig. 2. Effective contact resistivity and sheet resistivity vs P implant dose as measured with the *ContactSpot*

One key question concerning the strip sample preparation for the measurements is how wide to cut the strips. On one hand, even with laser scribing and snapping of strips from a cell, it can be quite challenging to snap strips much narrower than 5mm or so without breaking the strips, and it is always the case that one needs to be wary of samples with large ratios of perimeter length to area since recombination and shunting at edges can distort measurements. On the other hand, the standard TLM analysis assumes that each linear contact element is at a constant potential and that current flows uniformly between one contact and the next. For very wide strips with narrower fingers, the voltage drop down the length of the finger can be significant such that the current density between finger segments is stronger near where the current is injected than toward the ends of the fingers.

In the experiment below we systematically vary strip width for different samples to study this effect.

### III. EXPERIMENT

Experimental cells were fabricated on n-type monocrystalline wafers with B-implanted emitter layers on the front side and P implanted BSF layers on the rear side. Silver paste grids were printed and fired on both sides.

Subsequently the cells were laser scribed from the rear side into strips with widths of 5, 10, 15, 20, and 25 mm using a Coherent AVIA 355 nm laser with a galvo scanner system under the following conditions: 40 kHz pulse repetition frequency,  $\sim 290 \mu\text{J}/\text{pulse}$  (11.6 W), spot size 80-100  $\mu\text{m}$  diameter, write speed 50 mm/s, and each section was written 4 times. The strips were separated by snapping over a sharp edge, and Fig. 3 shows an image of separated strips of different widths.

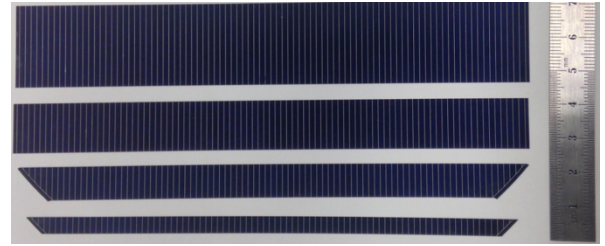


Fig. 3. Strips of different width prepared for the experiments

The contact resistivity was measured across each strip in a *ContactSpot* unit using a current injection level equivalent to a  $J_{sc}$  level of  $\sim 40 \text{ mA}/\text{cm}^2$ . We used a 3-finger TLM algorithm which involved curve fitting linear slopes and intercepts for 2 points on the resistance vs finger spacing plots. Fig. 4 shows a plot of  $\rho_{C\text{-eff}}$  across the full width of one strip. The collection of such data typical takes  $\sim 5 \text{ min}$ .

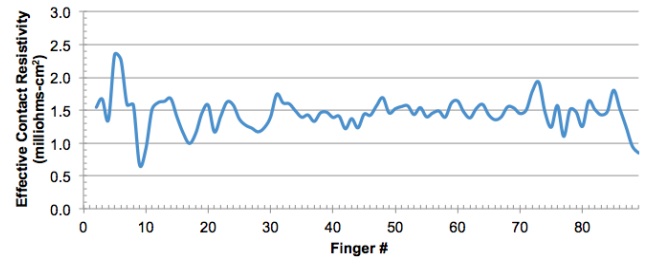


Fig. 4. Effective contact resistivity measurements across a full strip as measured with the *ContactSpot*

For each strip we calculated the median value of  $\rho_{C\text{-eff}}$  across all fingers in the strip and plotted the results vs. strip width. Fig. 5 shows the values for 4 different types of implanted layers. We consistently see higher values at both the 5mm and 25mm strip widths for both P and B implanted layers, with the lowest values at the 10 and 15mm strip widths.

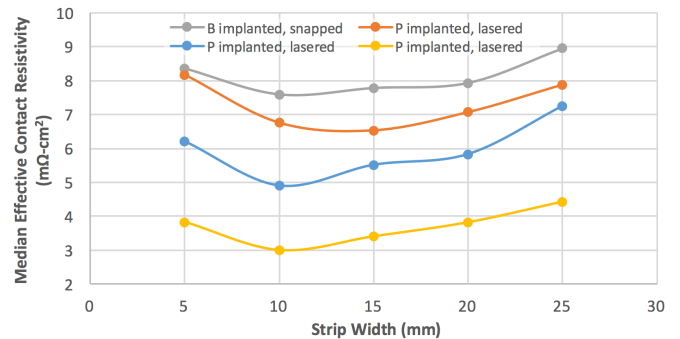


Fig. 5. Effective contact resistivity vs strip width for 4 different implanted layers

In another experiment we examined whether we could obtain accurate contact resistivity measurements without snapping strips from the cell. For some applications it can be more convenient to leave the full cell intact, especially when

mapping is being performed over large areas. Fraunhofer ISE has successfully performed mapping of unsnapped strips that were isolated with a dicing saw that cut half way through the depth of the cells [4], but we are not aware of any similar data using laser scribing for attempted isolation. We used the laser scribing parameters described above and in addition explored a case with shallower scribe depths by increasing the write speed to 100 mm/s. We applied these two conditions to both P and B implanted sides for a total of four cells. The results shown below in Table I indicate that only the heavier (slower) scribing condition was successful, with consistently very little change in  $\rho_{C-eff}$  before and after snapping the strips from the cell. However, under these deep scribing conditions, care has to be taken when handling the cells to prevent undesired snapping of the strips. When isolation of a strip is insufficient, current transport outside the strip leads to artificially high values of  $\rho_{C-eff}$ . The reason why the P-implanted BSF side was more challenging to isolate may be related to the fact that the wafer was n-type and thus most of the depth of the cell required isolation rather than just the thin surface-doped region. Still, a significant percentage of the datapoints were promising enough for the heavy scribing condition that better optimized conditions could be successful for the BSF side isolation. Presumably, P doped emitters on conventional p-type cells would be successfully isolated with these conditions as well. Since the laser is cutting through the fingers and the silicon, the effectiveness of any scribing condition may be influenced by the profile of the silver fingers.

TABLE I  
LASER ISOLATION OF STRIPS

Implant Side	Write speed (mm/s)	Distribution of the Relative % Decrease in Effective Contact Resistivity of Finger Segments After Snapping the Strip			
		< 2% change	2-5% change	5-20% change	>20% change
B	100	25%	0%	70%	5%
B	50	98%	3%	0%	0%
P	100	0%	0%	0%	100%
P	50	72%	3%	0%	24%

#### IV. DISCUSSION

For the narrower strips, the higher values of  $\rho_{C-eff}$  might be explained by shunt paths along the long edge of the strips. The severity of the shunts may explain some of the differences between different samples. The calculations assume that the voltage drop that we measure is all due to  $R_C$  and resistive losses from current flowing through the silicon. However, shunts could allow some of the current to find a

lower resistance path between the contacts. Presumably this effect will be stronger for wider contact spacings as the ratio of edge perimeter to fixed current injection level increases. In the TLM method the y-intercept value is influenced by the slope of the plotted resistance values vs contact spacing. By undermeasuring the voltage (and resistance) for wider contact spacings, the slope of the linear fit becomes lower (see Fig. 6), thus increasing the y-intercept point, and artificially increasing the calculation of  $R_C$ . In addition, the shunt paths may be voltage dependent, thus exacerbating the effect. It is possible that better optimized scribing conditions or treatment of the edges such as sanding could reduce the edge shunting effects. A similar argument may explain the higher values of  $\rho_{C-eff}$  seen for incomplete laser scribe isolation on unsnapped cell strips.

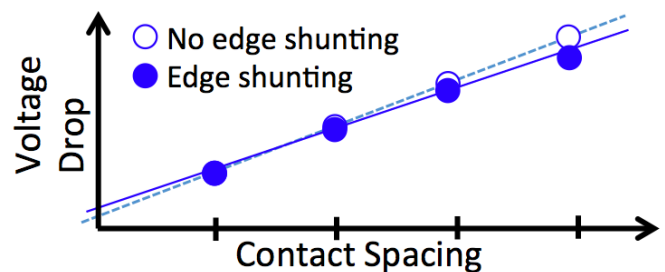


Fig. 6. Rollover effect in the TLM method leading to an overestimation of the y-intercept value

For wider strips, the current flow in the semiconductor will be more concentrated in the center region of the strip than near the strip edges due to the voltage drop across a long finger segment. This is depicted in Fig. 7. As fingers become narrower and less conductive, this effect will become stronger.

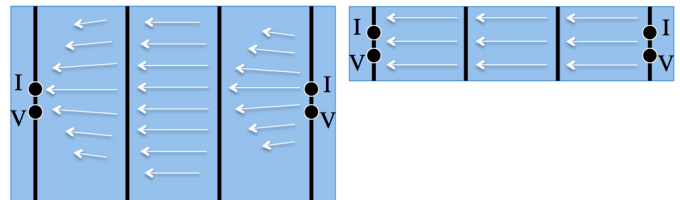


Fig. 7. Schematic depicting nonuniform current flow in a wide strip and uniform current flow in a narrow strip

When measuring close-spaced contacts we are overmeasuring the voltage drop (and thus the resistance in the TLM plot) since the current doesn't have a chance to spread out and utilize the full width of the strip. For wider spacings, the current spreads out more and better utilizes the strip width, and this effect again results in a lower slope in the TLM linear fit. The lower slope again translates into artificially high y-intercept and  $R_C$  values.

Another possible way of explaining the higher values seen with wide strips is that the effective width of the wide strips should be somewhat smaller than the geometrical widths.

When we multiply by the full width in the calculation of  $\rho_{C\text{-eff}}$  we are overestimating its value, and this may explain the trend toward higher values in the 25mm –wide strip cases.

Since the distortions on contact resistivity calculations from the above effects are to cause an overestimation, we take the minimum measured values to be most representative of the true value of the contact resistivity and suggest strip width values around ~10-15mm for P-doped layers on n-type wafers.

We have used TCAD and PSPICE programs to model the effects of strip width, edge shunting, voltage drop down the length of probed fingers, and the effect of current entering unprobed fingers [6]. These results confirm our experimental observations and are presented in a separate paper where we identify improved algorithms to be applied within the ContactSpot tool to produce more accurate and consistent results. These modified algorithms can extend the viability of cell-level TLM measurements as fingers become ever narrower in the future.

#### IV. CONCLUSIONS

We have shown that when the TLM method is applied to strips cut from solar cells, the choice of strips width is important. To measure the lowest and most accurate values, the strips should be cut to ~10-15mm in width for standard Ag paste fingers. Future optimization of the scribing technique to isolate the strips may lead to narrower strips being tolerated. As fingers become narrower and less conductive, artificially high values of contact resistivity will result from the measurement, and therefore we have identified TLM correction factors that take into account strip width and finger conductivity per unit length. We have identified laser scribing parameters that may allow contact resistivity measurements on the emitter side of the cells without the need to snap the strips from the cells, and this method of strip preparation may be quicker and more convenient, especially when mapping contact resistivity over large areas.

#### IV. ACKNOWLEDGEMENTS

We thank Karsten Bothe for helpful discussions. This material is based upon work supported in part by the U. S Department of Energy's Office of Energy Efficiency and Renewable Energy, in the Solar Energy Technologies Program, under Award Number DE-EE0004947.

#### REFERENCES

1. Janoch, R., Gabor, A.M., Anselmo, A. and Dube, C.E., "Contact resistance measurement-observations on technique and test parameters" *42nd IEEE Photovoltaic Specialist Conference (PVSC)*, (2015) p. 1

2. Yang, Y., Altermatt, P.P., Zhu, W., Liang, X. and Shen, H., "Analysis of industrial c-Si solar cell's front metallization by advanced numerical simulation" *Progress in Photovoltaics: Research and Applications*, 20(4), (2012) p. 490.
3. P.N. Vinod, "A modified TPP test structure for determining the specific contact resistance of the screen-printed Ag-metal contact of the silicon solar cell" *34th IEEE Photovoltaic Specialists Conference (PVSC)*, (2009) p. 1431.
4. Kontermann, S., Hörteis, M., Ruf, A., Feo, S. and Preu, R., "Spatially resolved contact-resistance measurements on crystalline silicon solar cells" *physica status solidi (a)*, 206(12), (2009) p. 2866.
5. D.K. Schroder, "Semiconductor Material and Device Characterization" Wiley-Interscience (2006).
6. G. Gregory, S. Guo, A. M. Gabor, A. M. Payne, K. O Davis, R. Janoch, A. Anselmo, "TCAD Modeling of TLM Contact Resistance Structures" to be published in *32nd European Photovoltaic Solar Energy Conference* (2017).